Reflection and transmission of x rays by graded interfaces

Ariel Caticha
Department of Physics, The University at Albany-SUNY, Albany, New York 12222
(Received 7 April 1995)

The reflection and transmission of x rays (and neutrons) by graded interfaces and surfaces of arbitrary profile are calculated by generalizing the approximation introduced by Nevot and Croce. The results apply also to the specular scattering by Gaussian and non-Gaussian random rough surfaces in the limit of short lateral correlation length. Two alternative approximation schemes are given: one involves the self-consistent calculation of the reflected field while the other imposes self-consistency for the transmitted field. The two alternatives give identical results for the reflection coefficient but not for the transmission coefficient. A third and better approximation is given by the geometric mean of the transmission coefficients obtained by the two alternatives above. Comparison with exact solutions for the special Epstein profile helps ascertain the accuracy of the approximations. The well-known peak of the transmitted amplitude for incidence at the critical angle is appreciably enhanced by grading the interface, and/or by roughness.

I. INTRODUCTION

Modern thin-film deposition methods have led to new synthetic materials with useful properties which are strongly correlated with the nature of the surfaces and interfaces. To satisfy the increasing demand for surface structural information a number of techniques have evolved, one of them being the scattering of x rays at grazing incidence.[1,2] Thus, quite apart from its intrinsic interest, there is a pressing need for reliable theories of reflection by complex surfaces.

The waves scattered by a real interface naturally separate into specular and nonspecular components. The specular or coherent waves are essentially what one would obtain if the inhomogeneities in the real interface are averaged out. This averaging procedure replaces the real rough interface by an equivalent, effective graded interface. For example, a rough surface with a Gaussian height distribution is replaced by an effective surface with a graded profile given by an error function. The real and the effective interfaces are not identical and this difference causes an additional scattering, which is the source of the nonspecular waves, also known as incoherent, or diffuse waves. Therefore, one important reason to calculate the specular reflection by graded interfaces is that this is a necessary first step in the calculation of scattering (specular *and* diffuse) by purely rough surfaces. The second motivation is, of course, that real interfaces may be both rough *and* graded simultaneously.

There is an extensive literature on specular and diffuse scattering by purely rough surfaces.[2–14] For x rays and neutrons the effect of roughness on the specular component can be taken into account by multiplying the Fresnel reflectivity of an ideal sharp and planar surface by a "static Debye-Waller" factor. The calculation of this factor has been carried out in many ways. For example, one may use the Rayleigh approximation[3,4]

$$r \approx r_s e^{-2q^2\sigma^2} \tag{1}$$

where r_s is the reflection coefficient for a sharp smooth surface, q is the normal component of the incident wave vector, and σ^2 is the mean-square roughness. This approximation is good for purely rough surfaces with very long lateral correlation lengths but fails for short correlation lengths particularly for angles of incidence close to or below the critical angle θ_c. Using the distorted-wave Born approximation[5,6] (DWBA) improves the description for small angles but fails for angles larger than a few times θ_c. For short lateral correlation lengths a better approximation, based on the self-consistent calculation of the scattered fields, was proposed by Nevot and Croce[7] (NC),

$$r \approx r_s e^{-2q\bar{q}\sigma^2} . \tag{2}$$

Here $\bar{q}$ is the normal component of the transmitted wave vector. This is similar to the Rayleigh result, Eq. (1), except within the region of total reflection where $\bar{q}$ becomes imaginary; it provides a reasonable description of both the low and the high angle regimes. Two other significant developments are a study of how the DWBA should be modified to reproduce the NC approximation by Pynn,[8] and an interpolation suggested by de Boer[9] between the Rayleigh and NC expressions to describe the regime of intermediate correlation lengths.

The simplicity of Eqs. (1) and (2) has led to their wide acceptance; the exploration of their validity has, however, been rather limited.[13,14] The transmission coefficients have received even less attention.

The NC approximation was developed for the special case of a sharply defined surface with Gaussian roughness. This leads to an effective graded interface described by an error-function profile. In this paper we generalize the method and calculate the specular reflection and transmission of x rays (and neutrons) directly for *graded interfaces of arbitrary profile.*[15] Our results apply also to the specular scattering by non-Gaussian rough surfaces, and to interfaces that may be both rough and diffuse.

0163-1829/95/52(13)/9214(10)/$06.00

The basic equations are set up in Sec. II. To solve them we offer two alternative approximation schemes. *A priori* there is no reason to prefer one over the other. The first involves the self-consistent calculation of the reflected field (Sec. III) while the second imposes self-consistency for the transmitted field (Sec. IV). The two schemes give identical results for the reflection coefficient, which suggests that this generalized NC approximation is reliable even for moderately thick transition layers. We find, however, that the two alternatives do not lead to the same expressions for the transmission coefficient. This disagreement can be a valuable indication of how far these approximations can be pushed. In general, this discrepancy is not a serious problem; after all, substrates are thick and the transmitted beams are not normally observed. There are, however, situations where the transmitted beam is observed indirectly. One may measure, for example, the effects on diffuse scattering,[11,16] or on the excitation of fluorescence,[17] or even on Bragg diffracted beams in multilayered structures,[18] where the transmission through upper layers is necessary to reach the deeper ones. To explore the reliability of these approximations we have considered in Sec. V the special case of zero absorption for arbitrary profiles, and also the special case of the Epstein (or hyperbolic tangent) profile[3,19] for which exact solutions are known. This leads us to suggest that a third, better approximation for the transmission coefficient is given by the geometric mean of the expressions obtained by the two alternatives above.

In Sec. VI the various approximations are compared numerically among themselves, and with the exact solutions when possible. We find that for the reflected waves the generalized NC calculation of the amplitude is very accurate even for very thick transition layers (say, about 40 Å), while the phase is calculated reliably only for transition layers of moderate thickness (say, less than 20 Å). For the transmitted waves we find that all three of our generalized NC approximations are reliable for both amplitude and phase for transition layers of moderate thickness. Above critical incidence our third NC approximation predicts the transmitted amplitude very accurately even for thick transition layers. As mentioned above, an important feature of the transmitted amplitude is that it has a pronounced peak at the critical angle. We find that, unlike the effect of absorption, the effect of grading the interface (and therefore, the effect of roughness as well) is to appreciably enhance this peak. Therefore, the peak itself contains useful surface structural information.

II. BASIC EQUATIONS

As mentioned above, whether one deals with a purely rough surface, a purely diffuse interface, or a combination of the two, as far as the specular scattering is concerned, they may all be replaced by equivalent graded interfaces. Consider, therefore, a graded interface described by the dielectric susceptibility $\chi(z)$ depending only on the normal coordinate z. An x-ray plane wave of vacuum wave number $K=\omega/c$ and polarized normally to the plane of incidence is incident at an angle θ to the surface. The electric field satisfies the wave equation

$$\left[\frac{d^2}{dz^2}+q^2+K^2\chi(z)\right]E(z)=0\ , \tag{3}$$

where $q=K\sin\theta$ is the component of the wave vector normal to the surface. Since $\chi(z)$ depends only on the normal coordinate z and not on the transverse coordinates x and y, the tangential component of momentum is conserved. This implies the reflection is specular. Let

$$\chi(z)=\chi_s(z)+\delta\chi(z)\ , \tag{4}$$

where

$$\chi_s(z)=\begin{cases}0 & \text{if } z<z_0\\ \chi_0 & \text{if } z>z_0\end{cases}$$

describes an ideally sharp interface between vacuum ($z<z_0$) and a medium ($z>z_0$) of susceptibility χ_0, and $\delta\chi$ represents the transition layer. Below we will exploit the fact that the separation of $\chi(z)$ into $\chi_s(z)$ and $\delta\chi(z)$ is quite arbitrary: even if our graded surface lies roughly at $z=0$ [one may, for example, impose $\chi(0)=\chi_0/2$], the choice of z_0 is not unique.

The reflection of neutrons is described by analogous equations with the electric field $E(z)$ replaced by the wave function, and the susceptibility $\chi(z)$ given in terms of the potential $V(z)$ by

$$\chi(z)=-\frac{V(z)}{(\hbar K)^2/2m}\ .$$

Equation (3) can be rewritten in integral form as

$$E(z)=E_s(z)+\int dz'G(z,z')K^2\delta\chi(z')E(z')\ , \tag{5}$$

where $E_s(z)$ and $G(z,z')$ are the field and the Green's function for an ideally sharp interface at $z=z_0$:

$$E_s(z)=\begin{cases}e^{iqz}+r_s e^{2iqz_0}e^{-iqz} & \text{for } z<z_0\ ,\\ t_s e^{i(q-\bar{q})z_0}e^{i\bar{q}z} & \text{for } z<z_0\ ,\end{cases} \tag{6}$$

and

$$G(z,z')=\begin{cases} G_1=\dfrac{i}{2q}\left[e^{iq|z-z'|}+r_s e^{2iqz_0}e^{-iq(z+z')}\right] & \text{for } z,z'<z_0 \\ G_2=\dfrac{i}{2\bar{q}}\left[e^{i\bar{q}|z-z'|}-r_s e^{-2i\bar{q}z_0}e^{i\bar{q}(z+z')}\right] & \text{for } z,z'>z_0 \\ G_3=\dfrac{i}{q+\bar{q}}e^{i(q-\bar{q})z_0}e^{i\bar{q}z-iqz'} & \text{for } z'<z_0<z \\ G_4=\dfrac{i}{q+\bar{q}}e^{i(q-\bar{q})z_0}e^{i\bar{q}z'-iqz} & \text{for } z<z_0<z' \end{cases} \tag{7}$$

where

$$r_s=\frac{q-\bar{q}}{q+\bar{q}} \quad \text{and} \quad t_s=\frac{2q}{q+\bar{q}} \tag{8}$$

are the Fresnel reflection and transmission coefficients of a sharp interface and $\bar{q}$ is the z component of the transmitted wave vector deep into the medium,

$$\bar{q}=(q^2+K^2\chi_0)^{1/2}\ . \tag{9}$$

In the Born approximation, $E_s(z)$ is taken as an incident plane wave e^{iqz}, and $G(z,z')$ is the vacuum Green's function, given by G_1 in Eq. (7), with $r_s=0$. The field $E(z')$ within the medium is also approximated by $e^{iqz'}$. This is justified at large incidence angles where the reflectivity is very low; it fails close to the critical reflection region. One obtains

$$r=-\frac{K^2}{4q^2}\frac{\chi'(2q)}{\chi_0}\ , \tag{10}$$

where

$$\chi'(Q):=\int\frac{d\chi(z)}{dz}e^{-iQz}dz\ . \tag{11}$$

Equation (10) is obviously flawed for small q; for larger values of q the approximation is, to the same order in χ_0, equivalent to

$$r=r_s\frac{\chi'(2q)}{\chi_0}\ . \tag{12}$$

For graded interfaces this is also inaccurate for low q, but at least, it is not divergent. We will refer to this expression, with the transmission coefficient given by $t=t_s$ as the Rayleigh approximation. For an error-function profile this leads to Eq. (1).

III. FIRST APPROXIMATION OF THE NEVOT-CROCE TYPE: SELF-CONSISTENT REFLECTED WAVE

We want to obtain approximate solutions to the integral equation (5). As was mentioned in the preceding section, one can take advantage of the arbitrariness of the location of the point z_0 that separates $\chi(z)$ into $\chi_s(z)$ and $\delta\chi(z)$. Suppose we choose $z_0\ll 0$, so that $\delta\chi(z)$ extends well into the vacuum (see Fig. 1); $\delta\chi(z)$ has sign opposite to that of $\chi_s(z)$ so that in the vicinity of z_0 they completely cancel out.

Consider the integral over $\delta\chi$ in the right-hand side of (5); for an appreciable part of the region of integration the unknown field $E(z')$ is just the field in vacuum. This suggests the following approximation: under the integral sign in Eq. (5) let

$$E(z')\approx e^{iqz'}+r\,e^{-iqz'} \tag{13}$$

where r is the unknown reflection coefficient we wish to calculate. But, for $z\ll 0$, the *exact* field is of the form (13). Therefore, for $z<z_0\ll 0$, Eq. (5) becomes

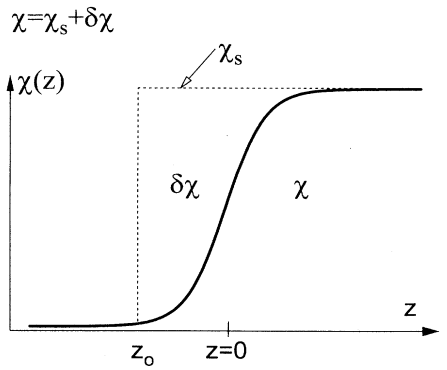

FIG. 1. The susceptibility profile $\chi(z)$ for a graded interface located at $z\approx 0$ showing the transition layer $\delta\chi(z)$ for the choice $z_0\ll 0$.

$$r\,e^{-iqz}=r_s e^{2iqz_0}e^{-iqz}+\int_{z_0}^{\infty}dz'G_4(z,z')K^2\delta\chi(z')(e^{iqz'}+re^{-iqz'}) \tag{14}$$

which, using Eqs. (7) and (8), allows us to solve for r in a self-consistent way. The integral in (14) is evaluated using

$$\int_{z_0}^{\infty}dz'\delta\chi(z')e^{iQz'}=\frac{\chi_0}{iQ}\left[e^{iQz_0}-\frac{\chi'(Q)}{\chi_0}\right], \tag{15}$$

where $\chi'(Q)$ is the Fourier transform of the derivative $d\chi/dz$ given in Eq. (11). Equation (15) can be verified by integrating the left-hand side by parts, replacing $d\delta\chi/dz$ by $d\chi/dz$ and using $z_0\ll 0$ to extend the lower limit of integration to $-\infty$.

We thus arrive at the first result of this paper: the self-consistent reflection coefficient for an arbitrary graded profile $\chi(z)$ is

$$r=r_s\frac{\chi'(\bar{q}+q)}{\chi'(\bar{q}-q)}\ . \tag{16}$$

The dependence on the arbitrarily chosen point z_0 has completely canceled out. For the special case of an error-function profile, Eq. (16) reproduces the Nevot-Croce result, Eq. (2).

We can now calculate the transmission coefficient t_1 *using the same approximation,* Eq. (13). For $z\gg 0$, Eq. (5) reads

$$t_1e^{i\bar{q}z}=t_se^{i(q-\bar{q})z_0}e^{i\bar{q}z}+\int_{z_0}^{\infty}dz'G_2(z,z')K^2\delta\chi(z')(e^{iqz'}+re^{-iqz'})\ . \tag{17}$$

Using Eqs. (7) and (8), dependence on z_0 again cancels out, and we obtain

$$t_1=t_s\frac{\chi'(q-\bar{q})}{\chi_0}\frac{1-r_s^2[\chi'(\bar{q}+q)/\chi'(\bar{q}-q)][\chi'(-\bar{q}-q)/\chi'(-\bar{q}+q)]}{1-r_s^2}\ . \tag{18}$$

Before analyzing these results let us consider a different choice of the point z_0.

IV. SECOND APPROXIMATION OF THE NEVOT-CROCE TYPE: SELF-CONSISTENT TRANSMITTED WAVE

Suppose we choose $z_0\gg 0$ (see Fig. 2) then the unknown field $E(z')$ within the integral in Eq. (5) is essentially the field that was transmitted past the graded interface into the bulk medium. This suggests the approximation

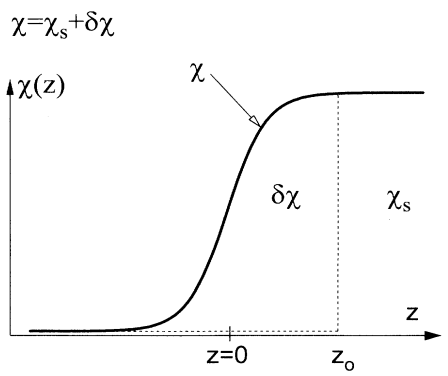

FIG. 2. The susceptibility profile $\chi(z)$ for a graded interface located at $z\approx 0$ showing the transition layer $\delta\chi(z)$ for the choice $z_0\gg 0$.

$$E(z')\approx t_2e^{i\bar{q}z'}\ , \tag{19}$$

where t_2 is the unknown transmission coefficient we wish to calculate. But, for $z\gg 0$, the *exact* field is of the form (19). Therefore, for $z>z_0\gg 0$, Eq. (5) becomes

$$t_2e^{i\bar{q}z}=t_se^{i(q-\bar{q})z_0}e^{i\bar{q}z}+\int_{-\infty}^{z_0}dz'G_3(z,z')K^2\delta\chi(z')t_2e^{i\bar{q}z'}\ , \tag{20}$$

where G_3 is given in Eq. (7), and the integral is similar to Eq. (15):

$$\int_{-\infty}^{z_0}dz'\delta\chi(z')e^{iQz'}=\frac{\chi_0}{iQ}\left[e^{iQz_0}-\frac{\chi'(Q)}{\chi_0}\right]. \tag{21}$$

The self-consistent solution for t_2 is

$$t_2=t_s\frac{\chi_0}{\chi'(\bar{q}-q)}\ . \tag{22}$$

As in the preceding section the reflection coefficient can now be calculated in the same approximation of Eq. (19). For $z\ll 0\ll z_0$, Eq. (5) becomes

$$r\,e^{-iqz}=r_se^{2iqz_0}e^{-iqz}+\int_{-\infty}^{z_0}dz'G_1(z,z')K^2\delta\chi(z')t_2e^{i\bar{q}z'}\ . \tag{23}$$

Using Eqs. (7), (8), and (22) and the identity (21), the calculation of r yields the same reflection coefficient we had before, Eq. (16). In words: whether we impose self-consistency of the reflected field or of the transmitted field, the result for r is the same. This is encouraging; it suggests the approximations for r are reliable. But t_1

differs from t_2. To study how good the approximations for t are it is convenient to examine some special cases.

V. APPLICATION TO SPECIAL PROFILES: AN IMPROVED TRANSMISSION COEFFICIENT

The first special case we consider is that of an ideally sharp interface at some arbitrary $z=z_a$. In this case our generalized Nevot-Croce approximations, Eqs. (16), (18), and (22) yield the exact results

$$r=(q-\bar{q}/q+\bar{q})e^{2iqz_a} , \tag{24}$$

and

$$t_1=t_2=2q/(q-\bar{q})e^{2i(q-\bar{q})z_0} . \tag{25}$$

This is not surprising; for a sharp interface the approximations (13) and (19) are exact.

The second example we consider is that of a graded interface of arbitrary profile but zero absorption, χ_0 real. In this case energy conservation leads to the identity

$$|r|^2+(\mathrm{Re}\bar{q}/q)|t|^2=1 , \tag{26}$$

which is not satisfied by Eq. (16) or either (18) or (22). Instead one can check that

$$|r|^2+(\mathrm{Re}\bar{q}/q)t_1t_2=1 . \tag{27}$$

This is a first indication that perhaps a better approximation to the transmission coefficient is given by

$$t_3=(t_1t_2)^{1/2} . \tag{28}$$

The argument above does not, of course, determine the phase of t_3.

The next example we consider is the Epstein profile,

$$\chi(z)=\chi_0/(1+e^{-2z/\sigma_E}) , \tag{29}$$

for which

$$\chi'(Q)/\chi_0=\frac{\pi}{2}\sigma_E Q\Big/\left[\sinh\left[\frac{\pi}{2}\sigma_E Q\right]\right] . \tag{30}$$

Equations (16), (18), and (22) give

$$r=\left\{\sinh\left[\frac{\pi}{2}\sigma_E(q-\bar{q})\right]\right\}\Big/\left\{\sinh\left[\frac{\pi}{2}\sigma_E(q+\bar{q})\right]\right\} , \tag{31}$$

$$t_1=t_s\frac{\left[\frac{\pi}{2}\right]\sigma_E(q-\bar{q})}{\sinh[(\pi/2)\sigma_E(q-\bar{q})]}\frac{1-r^2}{1-r_s^2} , \tag{32}$$

and

$$t_2=t_s\left\{\sinh\left[\frac{\pi}{2}\sigma_E(q-\bar{q})\right]\right\}\Big/\left[\frac{\pi}{2}\sigma_E(q-\bar{q})\right] . \tag{33}$$

The expression of Eq. (31) [but not Eqs. (32) and (33)] has been previously obtained by Hamilton and Pynn[13] by applying the DWBA directly to a rough surface with heights h distributed according to a $\mathrm{sech}^2(h/\sigma_E)$ probability distribution. Our derivation is for the graded interface allowing a direct comparison with the known exact solutions, r_E and t_E.[3,13,19] In terms of Eqs. (31)–(33) these exact solutions are

$$r_E=re^{i\phi_r} \quad \text{and} \quad t_E=(t_1t_2)^{1/2}e^{i\phi_t} , \tag{34}$$

where the factors $e^{i\phi_r}$ and $e^{i\phi_t}$ can be written in terms of Γ functions,

$$e^{i\phi_r}=\frac{\Gamma(1+iq\sigma_E)\Gamma[-(i/2)\sigma_E(q+\bar{q})]\Gamma[-(i/2)\sigma_E(q-\bar{q})]}{\Gamma(1-iq\sigma_E)\Gamma[(i/2)\sigma_E(q+\bar{q})]\Gamma[(i/2)\sigma_E(q-\bar{q})]} , \tag{35}$$

and

$$e^{i\phi_t}=\frac{\Gamma[1-(i/2)\sigma_E(q+\bar{q})]}{\Gamma[1+(i/2)\sigma_E(q+\bar{q})]}\left[\frac{\Gamma(1+iq\sigma_E)\Gamma(1+i\bar{q}\sigma_E)}{\Gamma(1-iq\sigma_E)\Gamma(1-i\bar{q}\sigma_E)}\right]^{1/2} . \tag{36}$$

A few comments are in order. *If there is no absorption and one is outside the total reflection region* ($\theta>\theta_c$) so that both q and $\bar{q}$ are real it is easy to see that $e^{i\phi_r}$ and $e^{i\phi_t}$ are pure phase factors. The generalized Nevot-Croce expressions for r and t are off by a phase but the reflectance and transmittance are reproduced exactly: $|r_E|^2=|r|^2$ and $|t_E|^2=|t_3|^2$. This constitutes further evidence in favor of Eq. (28). Within the total reflection region ($\theta\le\theta_c$)$\bar{q}$ is pure imaginary (for zero absorption) and one can see that $e^{i\phi_r}$ is still a pure phase factor but $e^{i\phi_t}$ is not, thus $|r_E|^2=|r|^2$ but $|t_E|^2\neq|t_3|^2$. If there is absorption then $|r_E|^2\neq|r|^2$ and $|t_E|^2\neq|t_3|^2$.

Whether there is absorption or not, and whether $\theta>\theta_c$ or $\theta\le\theta_c$, the important question is when are the factors $e^{i\phi_r}$ and $e^{i\phi_t}$ close to unity; the fact that Eqs. (24) and (25) are the exact results suggests that the requirement for the validity of the various Nevot-Croce approximations is that transition layers be thin. In fact, an expansion of Eqs. (35) and (36) in powers of $q\sigma_E$ shows that even powers cancel out and the leading order in the expansions of ϕ_r and ϕ_t is cubic in $q\sigma_E$.

As a final example we consider the error-function

profile

$$\chi(z)=\chi_0\left[1-\mathrm{erf}\left[\frac{z}{\sqrt{2\sigma^2}}\right]\right], \tag{37}$$

for which

$$\frac{\chi'(Q)}{\chi_0}=e^{-Q^2\sigma^2/2}. \tag{38}$$

The reflection and transmission coefficients given by Eqs. (16), (18), (22), and (28) are

$$r=r_s e^{-2q\bar{q}\sigma^2}, \tag{39}$$

$$t_1=t_s e^{-(\bar{q}-q)^2\sigma^2/2}\frac{1-r^2}{1-r_s^2}, \tag{40}$$

$$t_2=t_s e^{+(\bar{q}-q)^2\sigma^2/2}, \tag{41}$$

and

$$t_3=t_s\left[\frac{1-r^2}{1-r_s^2}\right]^{1/2}. \tag{42}$$

Equations (39) and (41) are the results which Nevot and Croce obtained for a Gaussian rough surface.[7] One can check that all t_1, t_2, and t_3 increase as σ increases. For t_2, Eq. (41), this is obvious. For t_1 and t_3 the increase is due to the lower value of r. Our previous considerations suggest that for angles above the critical angle t_3 is the best approximation while the original Nevot-Croce result t_2 overestimates the effect of σ (see the next section).

VI. NUMERICAL ANALYSIS OF THE VARIOUS APPROXIMATIONS

A straightforward way to understand the implications of the expressions for r and t in the previous sections is to plot them. First we consider the reflection and transmission of Cu $K\alpha$ radiation by a silicon surface with an Epstein profile, Eq. (29). The transition layer has been chosen to be rather thick ($\sigma_E=100\lambda/\pi\approx 49.08$ Å) in order to enhance the differences between various approximations. The layer thickness for "good" interfaces may be much smaller, the rms roughness σ of a smooth surface may be as small as a few angstroms. The reflectivities $|r|^2$ shown in Fig. 3 are calculated using Epstein's exact solution, Eqs. (34) and (35), the Rayleigh approximation, Eqs. (12) and (30), and the generalized Nevot-Croce approximation, Eq. (31). One sees that the NC curve agrees extremely well with the exact solution. As discussed in the preceding section this is what one expects when the effects of absorption are small. On the other hand, the Rayleigh approximation deviates appreciably (the plot uses a logarithmic scale) from the exact solution. Even at high angles where the reflectivity is low and one might expect a first Born approximation to be

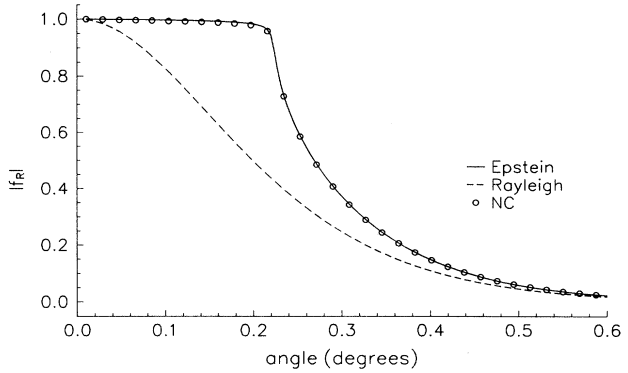

FIG. 4. The modulus of the static Debye-Waller factor for reflection $|f_r|=|r/r_s|$. The surface is the same as in Fig. 3. Solid line: Epstein's exact solution; dashed line: Rayleigh approximation; circles: generalized Nevot-Croce approximation.

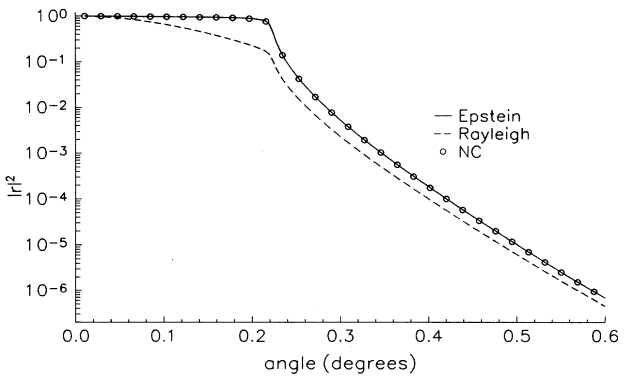

FIG. 3. Reflectivity $|r|^2$ of a silicon surface with an Epstein profile ($\sigma_E=49.08$ Å) for Cu $K\alpha$ radiation according to Epstein's exact solution (solid line), the Rayleigh approximation (dashed line), and our generalized Nevot-Croce approximation (circles).

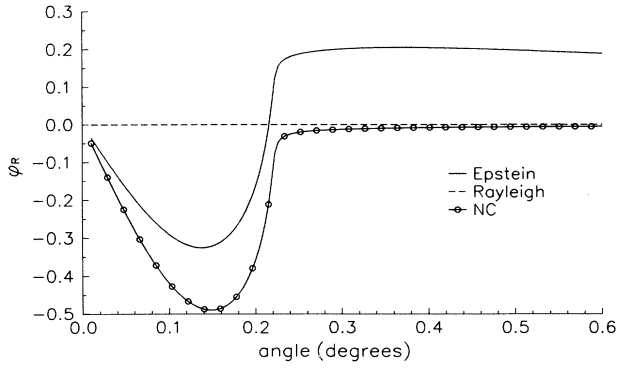

FIG. 5. The exact phase of the reflected beam differs appreciably from either the Nevot-Croce or Rayleigh approximations. The quantity plotted is $\phi_r=\arg(r/r_s)$ in radians. The surface has the same Epstein profile as in Fig. 3. Solid line: Epstein's exact solution; dashed line: Rayleigh approximation; solid line with circles: generalized NC approximation.

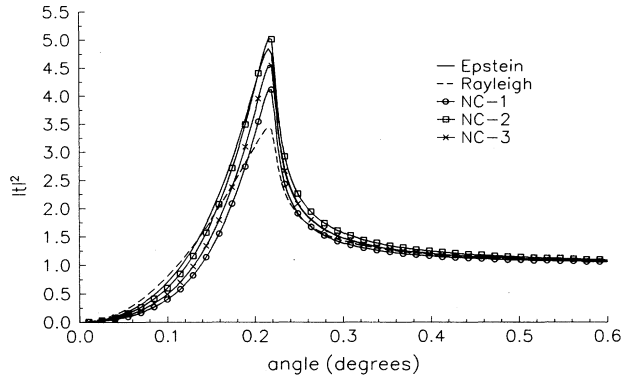

FIG. 6. The squared amplitude of the transmitted wave $|t|^2$ according to Epstein's exact solution (solid line), the Rayleigh approximation (dashed line), and the three generalized NC approximations (solid line with circles: $|t_1|^2$; solid line with squares: $|t_2|^2$; solid line with crosses: $|t_3|^2$). Same surface as in Fig. 3. Notice that the effect of grading the interface or of roughness is to enhance the amplitude at the critical angle.

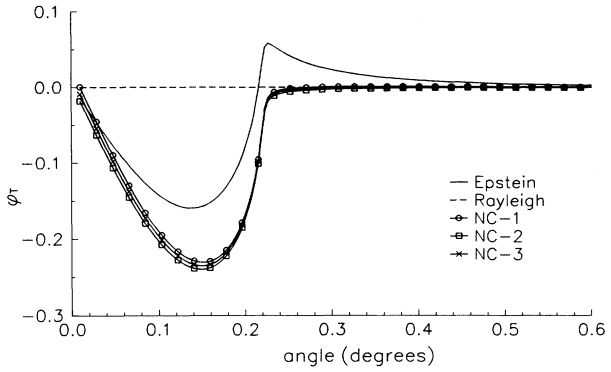

FIG. 8. The phase of the static Debye-Waller factor for the transmitted wave, $\phi_t = \arg(t/t_s)$ in radians. The surface has the same Epstein profile as in Fig. 3. Solid line: Epstein's exact solution; dashed line: Rayleigh approximation; solid line with circles, squares, and crosses: generalized NC approximations.

accurate we find a discrepancy of about a factor of 2. To exhibit the failure of the Rayleigh approximation in a different way we define the "static Debye-Waller" factor for reflection as $f_r = r/r_s$ and in Fig. 4 we plot its modulus $|f_r|$ in a linear scale. In this figure one can also barely see a very slight disagreement (because absorption effects are small) between the NC and the exact Epstein curves below the critical angle.

The generalized NC approximation reproduces extremely well the amplitude of the reflected wave even for thick transition layers. The phase of the reflected wave, however, is not predicted nearly as well (see Ref. 13 and the preceding section). The quantity plotted in Fig. 5 is the phase of the static Debye-Waller factor, $\phi_r = \arg(r/r_s)$, in radians. For this thick transition layer the exact phase differs appreciably from both the NC and Rayleigh approximations; for thinner layers we find that the agreement improves.

Next we consider the transmitted waves. In Fig. 6 we show the square of the amplitude of the transmitted wave $|t|^2$ calculated exactly [the Epstein solution, Eqs. (34) and (36), the Rayleigh approximation (which, as discussed at the end of Sec. II, we take as $t \approx t_s$), and the three generalized NC approximations Eqs. (32), (33), and (28)]. The most remarkable feature of these curves is the well-known peak of the transmitted amplitude at the critical angle. This effect is routinely observed indirectly through the Yoneda wings in diffuse scattering[11,16] and also

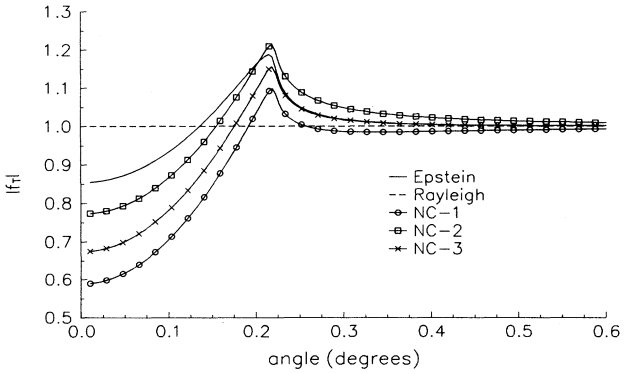

FIG. 7. The modulus of the static Debye-Waller factor for the transmitted wave $|f_t| = |t/t_s|$ according to Epstein's exact solution (solid line), the Rayleigh approximation (dashed line), and the three generalized NC approximations (solid line with circles: $|t_1|^2$; solid line with squares: $|t_2|^2$; solid line with crosses: $|t_3|^2$).

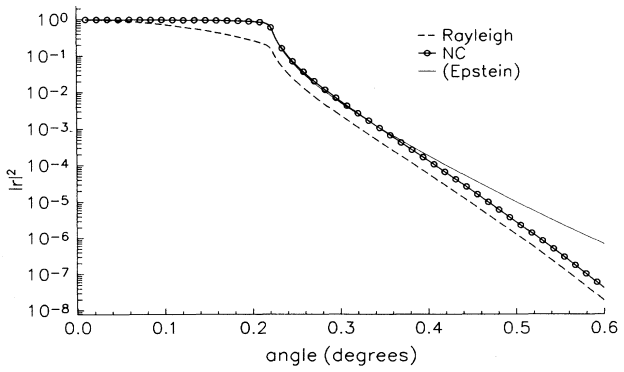

FIG. 9. Reflectivity $|r|^2$ of a silicon surface with an error-function profile ($\sigma = 39.16$ Å) for Cu $K\alpha$ radiation according to the Rayleigh approximation (dashed line) and the NC approximation (solid line with circles). Also shown is the exact reflectivity of the "best" Epstein match ($\sigma_E = 49.08$ Å).

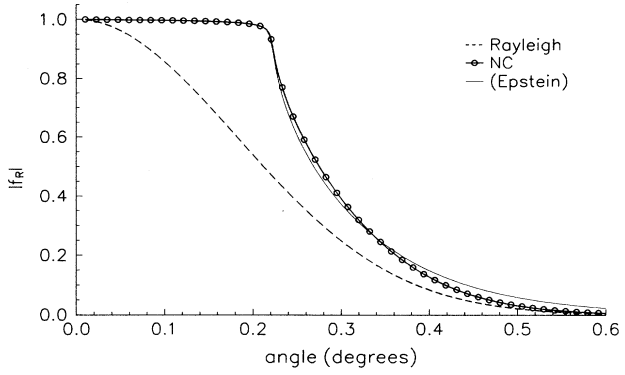

FIG. 10. The modulus of the static Debye-Waller factor for reflection $|f_r|=|r/r_s|$ for the error-function profile of Fig. 9. Dashed line: Rayleigh approximation; solid line with circles: NC approximation; solid line: "best" Epstein match (same curve as in Fig. 4).

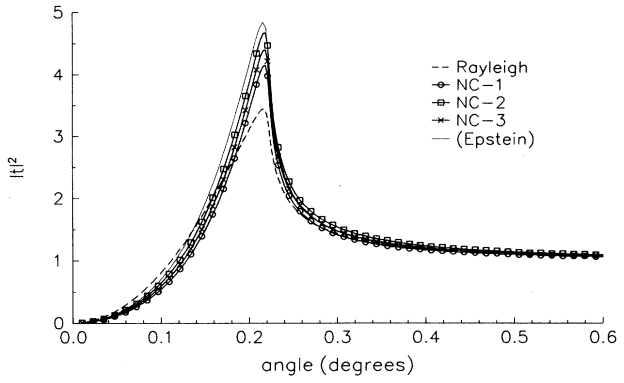

FIG. 12. The squared amplitude of the transmitted wave $|t|^2$ for the error-function profile of Fig. 9 according to the Rayleigh approximation (dashed line), the three generalized NC approximations (solid line with circles: $|t_1|^2$; solid line with squares: $|t_2|^2$; solid line with crosses: $|t_3|^2$), and the "best" Epstein match (same curve as in Fig. 6).

through an enhanced fluorescence signal when the incident beam is at the critical angle.[17] If there is no absorption the Fresnel formula gives a maximum value of $|t_s|^2=4$; with absorption this value is somewhat reduced (dashed curve). Epstein's exact solution (solid line) shows another remarkable and perhaps surprising feature: the effect of grading the interface, and therefore (see Sec. I), the effect of roughness also, is to enhance rather than reduce this peak at the critical angle. This enhancement effect is shown by all three generalized NC approximations. For angles above critical we see that the third NC approximation, $|t_3|^2$, is in remarkable agreement with the exact solution. Again, this is a consequence of low absorption effects (see preceding section). For angles below critical we see that the second NC approximation, $|t_2|^2$, is better.

Essentially the same information is displayed more clearly in Fig. 7 where we show the modulus of a static Debye-Waller factor for the transmitted wave $|f_t|=|t/t_s|$. Note that for angles above critical, $|t_3|^2$ is the best approximation, and that for large incidence angles (say, $\theta>1.5\theta_c$) the naive Rayleigh expression $|t_s|^2$ is better than either $|t_1|^2$ or $|t_2|^2$.

The phase of the static Debye-Waller factor for the transmitted wave, $\phi_t=\arg(t/t_s)$ is shown in Fig. 8. Note that within the total reflection region the phase of the transmitted wave beam differs appreciably from either the Nevot-Croce or Rayleigh approximations, while for larger angles (say, $\theta>2\theta_c$) all approximations agree; the phase of the transmitted wave is that given by the ideal Fresnel transmission through a sharp surface.

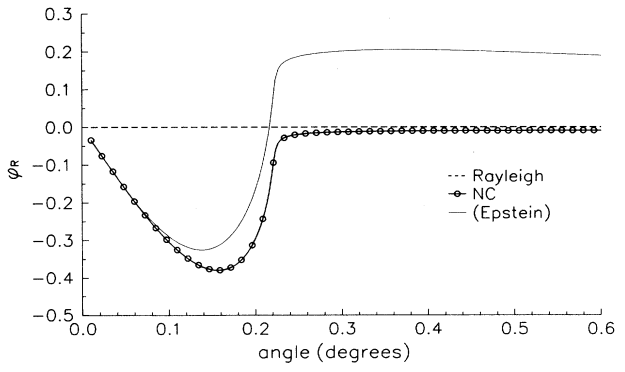

FIG. 11. The phase of the static Debye-Waller factor, $\phi_r=\arg(r/r_s)$ in radians for the error-function profile of Fig. 9. Dashed line: Rayleigh approximation; solid line with circles: NC approximation; solid line: "best" Epstein match (same curve as in Fig. 5).

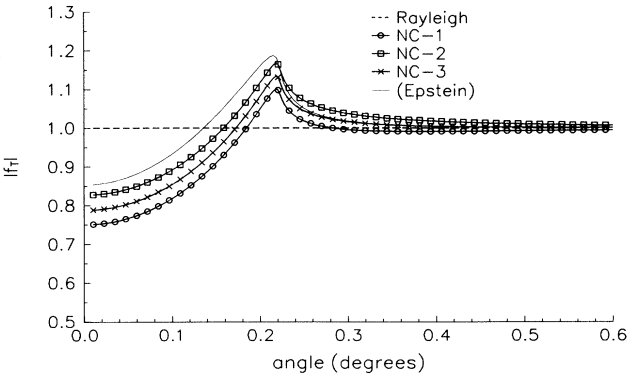

FIG. 13. The modulus of the static Debye-Waller factor for the transmitted wave $|f_t|=|t/t_s|$ for the error-function profile of Fig. 9 according to the Rayleigh approximation (dashed line), the three generalized NC approximations (solid line with circles: $|t_1|^2$; solid line with squares: $|t_2|^2$; solid line with crosses: $|t_3|^2$), and the "best" Epstein match (same curve as in Fig. 7).

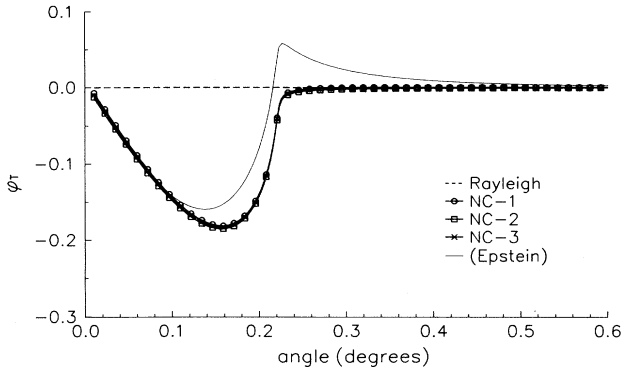

FIG. 14. The phase of the static Debye-Waller factor for the transmitted wave, $\phi_t = \arg(t/t_s)$ in radians for the error-function profile of Fig. 9 according to the Rayleigh approximation (dashed line), the three generalized NC approximations (solid line with circles: $|t_1|^2$; solid line with squares: $|t_2|^2$; solid line with crosses: $|t_3|^2$), and the "best" Epstein match (same curve as in Fig. 7).

Next we perform a similar analysis of the reflection and transmission of Cu $K\alpha$ radiation by a silicon surface with an error-function profile, Eq. (37). The difference is that now we do not have an exact solution against which our approximations may be compared. This problem is partially overcome by noting that the error-function and the Epstein profiles have quite similar shapes. Thus, for comparison we have included in Figs. 9–14, curves corresponding to the Epstein profile which "best" approximates the error function. This raises two questions: first, which is the best Epstein fit to an error function, and second, what is the effect of the slight differences between the two profiles?

The first question does not have a unique answer. Below we adopt the criterion of Ref. 14 according to which the "best" Epstein profile is chosen to have the same midpoint slope (i.e., slope at $z=0$) as the error-function profile. This gives $\sigma_E = 2\sigma/\pi \approx 0.8\sigma$. For an alternative criterion see Ref. 4.

The answer to the second question requires some care. One may reasonably expect that the small difference $\delta\chi$ between the two profiles will itself only contribute with a small amount of scattering (except at zero angle). The reflections from the two profiles must therefore be in close agreement except in those regions where the reflection by either profile is so weak that the small contribution due to $\delta\chi$ ends up being comparable and perhaps even dominant. Thus the answer is that we expect the reflections to disagree for large incidence angles. A similar effect has been found to occur in the far tails of Bragg diffraction peaks.[20]

We have chosen the thickness of the transition layer (the rms roughness), $\sigma = 39.16$ Å, so that the corresponding Epstein layer thickness is the same as in Figs. 3–8 ($\sigma_E = 49.08$ Å).

The reflectivities $|r|^2$ in Fig. 9 are calculated using the NC approximation, Eq. (39), and the Rayleigh approximation, Eqs. (12) and (38). Also shown is the reflectivity of the "best" Epstein match (same curve as in Fig. 3) which agrees well with the NC curve in the region where they are supposed to agree, namely at low angles. This is evidence of the reliability of the NC approximation. The disagreement at larger angles is as expected. The failure of the Rayleigh approximation is shown in Fig. 9 and also in Fig. 10, where we graph the modulus $|f_r|$ of the static Debye-Waller factor ($f_r = r/r_s$) in a linear scale. Note the slight difference between the NC approximation and its Epstein match. Figure 11, which shows the phase of the "static Debye-Waller" factor, $\phi_r = \arg(r/r_s)$, is similar to Fig. 5. For this thick transition layer neither the NC nor Rayleigh approximations are accurate; for thinner layers the accuracy improves.

Figures 12–14 show the square of the amplitude of the transmitted wave $|t|^2$, the modulus of a static Debye-Waller factor for the transmitted wave $|f_t| = |t/t_s|$, and its phase $\phi = \arg(t/t_s)$, for the same error-function profile. These are calculated using Eqs. (39)–(42). Also shown is the "best" Epstein match. These figures are closely analogous to Figs. 6–8 and so are our comments: The transmitted amplitude peaks at the critical angle; this peak is enhanced by either grading the interface, or equivalently, by roughness. Above critical incidence the best approximation is $|t_3|^2$; below critical incidence $|t_2|^2$ is somewhat better. All NC approximations are equivalent as far as the phase of the transmitted waves is concerned; they are expected to be accurate only for thin transition layers. For large incidence angles (say, $\theta > 2\theta_c$) the naive Rayleigh expression t_s (the Fresnel expression for a sharp surface) is accurate.

ACKNOWLEDGMENTS

Valuable discussions with J. Kimball and D. Bittel are gratefully acknowledged. This work was partially supported by the New York State Science and Technology Foundation through the N.Y.S. Center for Advanced Technology in Thin Films and Coatings.

[1] G. Parratt, Phys. Rev. **95**, 359 (1954).

[2] *Surface X-Ray and Neutron Scattering*, edited by H. Zabel and I. K. Robinson (Springer-Verlag, Berlin, 1992).

[3] P. Beckmann and A. Spizzichino, *The Scattering of Electromagnetic Waves from Rough Surfaces* (Artech house, Norwood, MA, 1987); J. Lekner, *Theory of Reflection of Electromagnetic and Particle Waves* (Martinez Nijof, Dordrecht, Holland).

[4] D. G. Stearns, J. Appl. Phys. **65**, 491 (1989); **71**, 4286 (1992); A. V. Vinogradov *et al.*, Sov. Phys. JETP **62**, 1225 (1985); **67**, 1631 (1988).

[5] S. K. Sinha *et al.*, Phys. Rev. B **38**, 2297 (1988).

[6]V. Holy *et al.*, Phys. Rev. B **47**, 15 896 (1993).
[7]L. Nevot and P. Croce, Rev. Phys. Appl. **15**, 761 (1980).
[8]R. Pynn, Phys. Rev. B **45**, 602 (1992).
[9]D. K. G. de Boer, Phys. Rev. **49**, 5817 (1994).
[10]J. B. Kortright, J. Appl. Phys. **70**, 3620 (1991).
[11]W. Weber and B. Lengeler, Phys. Rev. B **46**, 7953 (1992).
[12]J. C. Kimball and D. Bittel, J. Appl. Phys. **74**, 887 (1993).
[13]W. A. Hamilton and R. Pynn, Physica B **173**, 71 (1991).
[14]D. Bahr, W. Press, R. Jebasinksi, and S. Mantl, Phys. Rev. B **47**, 4385 (1993).
[15]Some of the present results are briefly mentioned in A. Caticha, Opt. Soc. Am. Tech. Digest **6**, 56 (1994).
[16]Y. Yoneda, Phys. Rev. **131**, 2010 (1963).
[17]R. S. Becker, J. A. Golovchenko, and J. R. Patel, Phys. Rev. Lett. **50**, 153 (1983); W. van den Hoogenhof and D. K. G. de Boer, Spectrochim. Acta **48B**, 277 (1993); B. Lengeler and M. Hüppauff, Fresenius Z. Anal. Chem. **346**, 155 (1993).
[18]A. Caticha, Proc. Soc. Opt. Eng. SPIE **1740**, 81 (1992).
[19]P. S. Epstein, Proc. Natl. Acad. Sci. U.S.A. **16**, 627 (1930).
[20]A. Caticha, Phys. Rev. B **47**, 76 (1993); **49**, 33 (1994).